



Effect of Si doping on the strain and defect structure of GaN thin films

L.T. Romano^{a,*}, C.G. Van de Walle^a, B.S. Krusor^a, R. Lau^a, J. Ho^a, T. Schmidt^a, J.W. Ager III^b, W. Götz^c, R.S. Kern^c

^aXerox Palo Alto Research Center, 3333 Coyote Hill Road, Palo Alto, CA 94304, USA

^bMaterials Sciences Division, Lawrence Berkeley National Laboratory, CA 94720, USA

^cHewlett-Packard Company, Optoelectronics Division, San Jose, CA 95131, USA

Abstract

The amount of strain was measured in GaN films using X-ray diffraction, Raman, and curvature techniques as a function of film thickness and the Si doping concentration. It was found that for a doping concentration of 2×10^{19} , the threshold thickness for crack formation was about 2.5 μm . Transmission electron microscopy observations showed that cracking proceeds without plastic deformation (i.e., no dislocation motion), and occurs catastrophically along the low-energy $\{1 \bar{1} 0 0\}$ cleavage plane of GaN. © 1999 Elsevier Science B.V. All rights reserved.

Keywords: Residual stress; GaN films; Dislocations

1. Introduction

Residual strain in the III–V nitrides has been observed previously [1–5] and found to limit the alloying and doping concentrations necessary for optoelectronic devices [6,7]. Raman and X-ray diffraction studies performed on Si-doped GaN films have shown that the residual compressive strain decreased with increasing Si concentration [5]. Based on transmission electron microscopy (TEM) studies, Ruvimov et al. suggested that the strain relief for moderately doped Si samples ($\sim 3 \times 10^{18} \text{ cm}^{-3}$) was due to the formation of dislocations in the basal plane [3].

In this paper the relationship between the extended defect structure and strain is studied in order to understand the mechanism of crack formation in GaN films. Films doped with Si were measured as a function of both the doping concentration [Si] and film thickness t and compared with the microstructure. The films were grown

by metal organic vapor deposition on (0 0 0 1) sapphire substrates up to 2.5 μm thick. Most of the samples were prepared by first depositing a low-temperature (LT) GaN buffer layer, followed by 100 nm of a high-temperature (HT) undoped layer, then introducing silane to begin the growth of the doped layer (A samples). Some of the 2 μm thick films were prepared by introducing the silane directly after growth of the LT buffer layer (B samples). Hall and secondary ion mass spectrometry (SIMS) were used to determine the carrier concentration and [Si]. In all the samples the agreement between the [Si] and carrier concentration indicated that all the Si was electrically active and therefore inferred to reside on the Ga site.

Strain was measured by using Raman, curvature, and X-ray diffraction (XRD) measurements. Raman study was measured by the shift in the E2 phonon with a lateral spatial resolution of 1 μm as discussed previously [4]. The a and c lattice constants were measured by XRD using the (1 0 $\bar{1}$ 5) and (0 0 0 2) reflections, respectively, and compared to values for bulk single crystal to determine the strain ($a_0 = 3.1876$ and $c_0 = 5.1846$ from porowski [8]). Strain from curvature measurements was calculated using the Stoney equation [9]. Atomic force microscopy (AFM), scanning (SEM) and transmission

* Corresponding author. Tel.: +1-650-812-4167; fax: +1-650-812-4140.

E-mail address: romano@parc.xerox.com (L.T. Romano)

electron microscopy (TEM) were used to measure the roughness and structure of the material. TEM samples were prepared in the usual way by mechanically thinning and ion milling to electron transparency.

2. Results

Fig. 1 shows the residual strain measured by Raman, curvature, and XRD as a function of Si doping. The strain is found to increase with both the film thickness and [Si]. At low [Si], the films are in compression which is expected to occur on cooling due to the difference in thermal expansion coefficients between GaN and sapphire. However, as the Si concentration increases the films are found to be in tensile stress. For $t = 1.0 \mu\text{m}$ the crossover from compressive to tensile strain is observed to occur at $[\text{Si}] \approx 10^{19} \text{cm}^{-3}$. The crossover for $t = 2.0 \mu\text{m}$ occurs at $[\text{Si}] \approx 10^{18} \text{cm}^{-3}$. The highest tensile strain ($\epsilon = 0.025$) was measured for $t = 2.5 \mu\text{m}$ at $[\text{Si}] = 2 \times 10^{19} \text{cm}^{-3}$. The strains measured by the various techniques were in fairly good agreement for all the Si concentrations. Some exceptions were noted at the highest [Si] where cracking was also observed. The reason for this is related to the spatial resolution of the Raman probe and the difference in the strain near and away from the cracks as discussed below.

Cracking was present in films with a doping level of $2 \times 10^{19} \text{cm}^{-3}$ for $t \geq 2 \mu\text{m}$. Subsurface cracking occurred for films with $t = 2 \mu\text{m}$ whereas cracks extended to the surface for films with $t = 2.5 \mu\text{m}$. The cracking occurred on the prismatic $\{1 \bar{1} 0 0\}$ cleavage planes [10] of the GaN (i.e., parallel to the growth direction). The subsurface cracking suggests that the films cracked during growth at high temperature. Fig. 2a is a TEM micrograph of a subsurface crack in a $2.0 \mu\text{m}$ thick B film. The

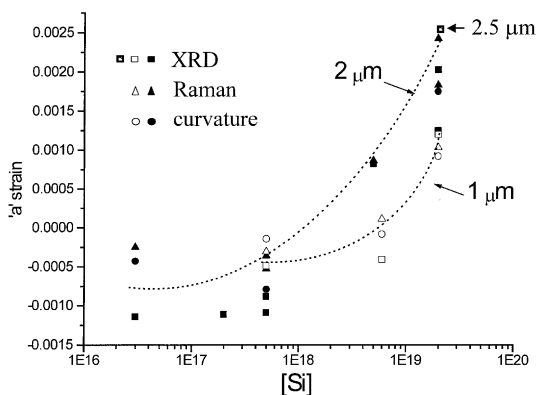


Fig. 1. The residual strain from Raman, curvature, and XRD measurements as a function of Si doping for $t = 1.0 \mu\text{m}$ (unfilled symbols), $2.0 \mu\text{m}$ (filled symbols), and $2.5 \mu\text{m}$ (patterned symbol).

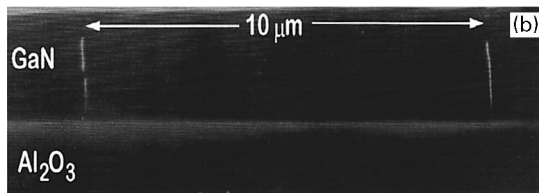
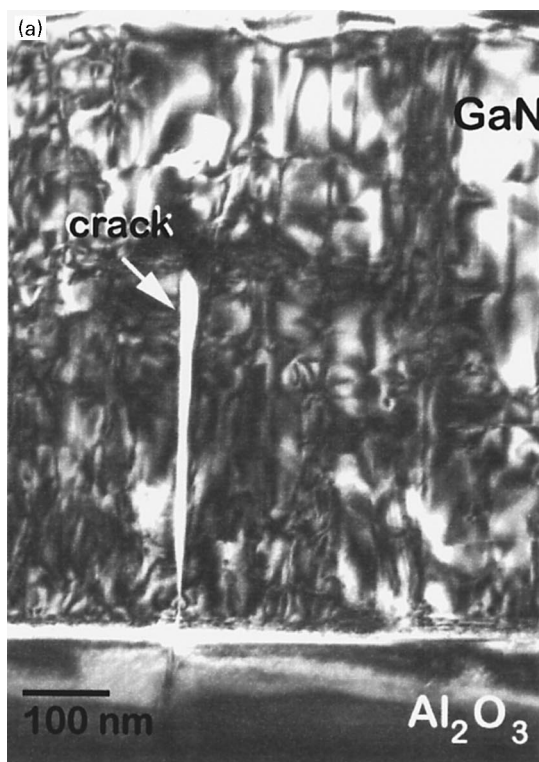


Fig. 2. (a) TEM micrograph of a subsurface crack in a $2.0 \mu\text{m}$ thick B film. (b) lower TEM magnification of the same film showing the separation between two subsurface cracks.

crack extends into the film/substrate interface and there are no additional dislocations observed near the crack. This suggests that plastic deformation does not take place to promote crack formation. The widest part of the crack is $\Delta L \sim 50 \text{nm}$ and from Fig. 2b, the average crack spacing is shown to be $L \sim 10 \mu\text{m}$. The amount of strain ϵ that has been relieved by the formation of the crack is $\epsilon = \Delta L/L = 0.005$.

The surface of the overgrown cracks is found to be higher than the region of the away from the cracks. The AFM image in Fig. 3 shows lines of lighter contrast which correspond to the position of the cracks below the surface. A line scan taken across the lighter contrast regions indicates that the surface above the crack is $\sim 15\text{--}20 \text{nm}$ higher compared to the surrounding region which has a root mean square (RMS) roughness of 3nm .

The surface cracks on the 2.5 μm thick films occurred at larger separation distances than the subsurface cracks and were found to initiate at pits or irregularities on the surface. They were also found to be preferentially on the $\{1\bar{1}00\}$ planes. Raman measurements showed variations in the strain depending on the position of the probe relative to the crack. The measurements were taken linearly at 2 μm intervals on either side of the crack. Near the crack, the film was found to be in a small amount of compressive strain (0.05%) compared to a maximum tensile strain of 0.16% measured 100 μm from the crack. The compressive strain near the crack is due to the residual strain from cooling to room temperature. The strain becomes tensile at a position 20 μm from the crack which indicates that the strain relief induced by the crack occurs locally.

Small differences in strain were measured in films with [Si] at 2×10^{19} prepared with and without the undoped prelayer. The films with the undoped prelayer (samples A) had a lower tensile strain compared to the B films (no prelayer). This may be due to the difference in microstructure observed in the TEM (not shown). For samples B, a region containing basal plane dislocations extended approximately 1 μm above the LT buffer layer (i.e., half the total film thickness). The presence of these dislocations may have introduced larger strains in the material. For the A samples, no basal plane dislocations were generated at the doped interface. Instead threading dislocations that were generated in the undoped prelayer extended unperturbed into the doped portion of the film.

3. Discussion

The origin of the increase in tensile strain with Si doping is puzzling. We have shown elsewhere that the effect of incorporating Si in the GaN lattice (substituting on a Ga site) has no net effect on the lattice constant of the GaN lattice [11], if both the size effect and the deformation-potential effect are taken into account. The size effect would result in a net contraction of the lattice, since the Si–N bond length is smaller than the Ga–N bond length. However, for the doping concentrations used in this study, the change in lattice constant due to the size effect is an order of magnitude smaller than the strains we observe. In addition by taking into account that the Si is electrically active (the SIMS and Hall measurements indicated that the Si and electron concentrations were in good agreement up to $2 \times 10^{19} \text{ cm}^{-3}$), the deformation-potential effect would lead to a net expansion of the lattice. The size effect and deformation-potential effects have similar magnitudes but are of opposite sign, resulting in no net change in strain with the addition of Si.

The observed changes in tensile strain when Si is incorporated can therefore not be attributed to a change in the lattice constant due to silicon. Silicon must therefore play a different role, presumably related to plastic deformation (or lack thereof). An understanding of this process would require better insight into the stress experienced by the film at the growth temperature, an issue that is only beginning to be explored. Recently, Hearne et al. reported in situ wafer curvature measurements that show

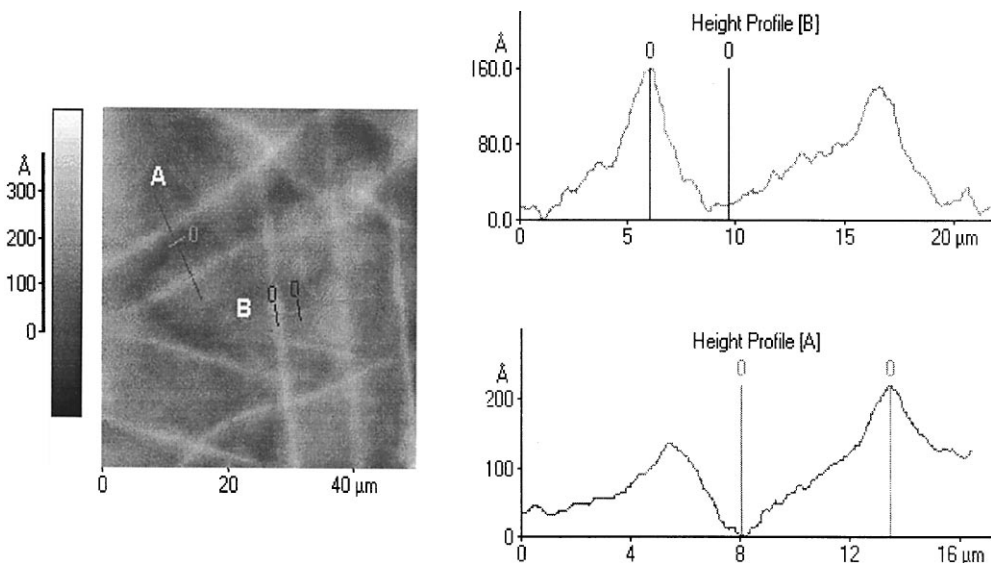


Fig. 3. (a) AFM micrograph of the surface of the same film in Fig. 2. (b) Line scans of the AFM image are taken through the regions of different contrast.

that tensile strains occur in GaN films at the growth temperature [9]. We suggest that this tensile strain may be related to the crystallite coalescence model developed recently by Nix and Clemens [12]. Their model shows that when the crystallite size decreases, the tensile stress increases. To address this issue we performed AFM measurements on 20 nm thick films grown over a 100 nm undoped layer. It was found that for $[\text{Si}] = 5 \times 10^{17} \text{ cm}^{-3}$ the RMS roughness was 5.5 nm compared to 11.0 nm for $[\text{Si}] = 2 \times 10^{19} \text{ cm}^{-3}$. It is possible that gaps on the growing GaN surface, due to the roughness, coalesce in a similar way as the crystallites described in the model by Nix and Clemens. Therefore increasing the roughness of the surface would be analogous to decreasing the crystallite size and therefore lead to higher tensile strains. Limited surface diffusion of atoms on the growing surface would then attach to the strained crystal at their point of arrival, and the film would grow in a strained state.

4. Conclusions

Crack formation in GaN films doped with Si was studied by measuring the strain and comparing to the microstructure. The strain was found to increase with film thickness and Si concentration. Crack formation along the $\{1\ 1\ 0\ 0\}$ cleavage planes was found to be the major strain relief mechanism and occurred without creating additional dislocations. This suggests that plastic deformation is difficult in these materials at the temperatures used during growth. It was proposed that the increase in tensile stress with increasing $[\text{Si}]$ may be related to the presence of tensile stress due to crystallite coalescence. The surface roughness increased with Si concentration, corresponding to an increased tensile

stress by invoking a modified view of a coalescence model established recently by Nix and Clemens [12].

Acknowledgements

This work was supported partially by DARPA MDA972-96-3-0014.

References

- [1] K. Hiramatsu, T. Detchprohm, I. Akasaki, *Jpn. J. Appl. Phys.* 32 (1993) 1528.
- [2] C. Kesielowski, J. Kruger, S. Ruvimov, T. Suski, J.W. Ager III, E. Jones, Z. Liliental-Weber, M. Rubin, E.R. Weber, M.D. Bremser, R.F. Davis, *Phys. Rev. B* 54 (1996) 17745.
- [3] S. Ruvimov, Z. Liliental-Weber, T. Suski, J.W. Ager III, J. Washburn, J. Krueger, C. Kesielowski, E.R. Weber, H. Amano, I. Akasaki, *Appl. Phys. Lett.* 69 (1996) 990.
- [4] J.W. Ager III, T. Suski, S. Ruvimov, J. Krueger, G. Conti, E.R. Weber, M.D. Bremser, R.F. Davis, C.P. Kuo, *Mater. Res. Soc.* 449 (1997) 775.
- [5] I. Lee, I. Choi, C. Lee, E. Shin, D. Kim, S.K. Noh, S. Son, K. Lim, H.J. Lee, *J. Appl. Phys.* 83 (1998) 5787.
- [6] S. Nakamura, T. Mukai, M. Senoh, *Jpn. J. Appl. Phys. Part 1* 31 (1992) 2883.
- [7] D.P. Bour, M. Kneissl, L.T. Romano, M.D. McCluskey, C.G. Van de Wall, B.S. Krusor, R.M. Donaldson, J. Walker, C.J. Dunrowicz, N.M. Johnson, *IEEE J. Sel. Top. Quantum Electron.* 4 (1998) 498.
- [8] S. Porowski, *J. Crystal Growth* 189/190 (1998) 153.
- [9] S. Hearne, E. Chason, J. Han, J.A. Floro, J. Figiel, J. Hunter, H. Amano, I.S.T. Tsong, *Appl. Phys. Lett.*, 1999.
- [10] J.E. Northrup, J. Neugebauer, *Phys. Rev. B* 53 (1996) R10477.
- [11] L.T. Romano, C.G. Van de Walle, J.A. Ager III, W. Gotz, S.A. Kern, in preparation.
- [12] W.D. Nix, B.M. Clemens, *J. Mater. Res.* 14 (1999) 3467.